

# Chaos identification through the auto-correlation function indicator (*ACFI*)

Valerio Carruba<sup>1</sup>, Safwan Aljbaae<sup>2</sup>, Rita C. Domingos<sup>3</sup>,  
Mariela Huaman<sup>4</sup> and William Barletta<sup>1</sup>

<sup>1</sup>São Paulo State University (UNESP),  
Guaratinguetá, SP, 12516-410, Brazil  
email: [valerio.carruba@unesp.br](mailto:valerio.carruba@unesp.br)

<sup>2</sup>National Space Research Institute (INPE),  
C.P. 515, 12227-310, São José dos Campos, SP, Brazil

<sup>3</sup>São Paulo State University (UNESP),  
São João da Boa Vista, SP, 13876-750, Brazil

<sup>4</sup>Universidad tecnológica del Perú (UTP),  
Cercado de Lima, 15046, Perú

**Abstract.** Close encounters or resonances overlaps can create chaotic motion in small bodies in the Solar System. Approaches that measure the separation rate of trajectories that start infinitesimally near, or changes in the frequency power spectrum of time series, among others, can discover chaotic motion. In this paper, we introduce the *ACF* index (*ACFI*), which is based on the auto-correlation function of time series. Auto-correlation coefficients measure the correlation of a time-series with a lagged duplicate of itself. By counting the number of auto-correlation coefficients that are larger than 5% after a certain amount of time has passed, we can assess how the time series auto-correlates with each other. This allows for the detection of chaotic time-series characterized by low *ACFI* values.

**Keywords.** Celestial mechanics; Asteroid Belt; Chaotic Motions; Statistical Methods.

---

## 1. Introduction

Fidelity, which measures the degree of similarity between two quantum states, has been employed to detect chaotic behavior in quantum computing [Frahm \*et al.\* \(2004\)](#), [Pellegrini & Montangero \(2007\)](#), [Lewis-Swan \*et al.\* \(2019\)](#). In the saw-tooth map, [Pellegrini & Montangero \(2007\)](#) determined fidelity values for quantum pure states in chaotic and integrable dynamics. In general, fidelity began at one, decreased until it reached a saturation point, and then oscillated about it. The saturation value for chaotic dynamics was substantially nearer to zero than for integrable systems, permitting the two forms of behavior to be distinguished.

In this research, we present a study about detecting chaotic behavior using the auto-correlation function. The correlation coefficient  $R$  between two time-series, as described by [Pearson \(1895\)](#), indicates how strong the association is.  $R$  near to 1 indicates strongly correlated series,  $R$  close to -1 indicates anti-correlated series, and  $R \simeq 0$  indicates uncorrelated series †.

The auto-correlation function (*ACF*) is obtained by computing values of  $R$  for the series with a lagged copy of itself. In essence,  $R$  values are computed for the series at

† Contrary to the case of quantum fidelity, anti-correlated series can have negative  $R$  values.

lag 0 in relation to the series at lag 1, 2, and so on. *ACF* depicts a range of  $R$  values connected with various time-lags. Most  $R$  values will be close to 1 for substantially auto-correlated time-series. Unpredictable series, such as white noise, would display the majority of  $R$  values near to zero once a sufficient amount of time has passed. After some time delay, which is a free parameter of the method, we can count the fraction of auto-correlation coefficients that are larger than the 5% value, which is commonly used for auto-regressive functions to set the null hypothesis level of negligible correlation. This new approach is called *ACFI*, which stands for auto-correlation function index. To test *ACFI*, in this work we will apply it to the well-understood Hénon-Heiles dynamical system Skokos *et al.* (2016), and compare its outcome to those of other chaos indicators, like the Smaller Alignment Index (*SALI*) approach Skokos *et al.* (2004).

## 2. Methods

Correlation coefficients can be defined in a variety of ways, but Pearson's approach is the most frequently used (Pearson (1895)). If the  $i$ -th term of the series in  $x$  and  $y$  is defined as  $x_i$  and  $y_i$ , then:

$$R = \frac{\text{cov}(X, Y)}{\sigma_X \sigma_Y}, \quad (2.1)$$

where  $\text{cov}(X, Y)$  denotes the covariance between the two series, which is defined as:

$$\text{cov}(X, Y) = \frac{1}{N^2} \sum_{i=1}^N \sum_{j=1}^N \frac{1}{2} (x_i - x_j)(y_i - y_j). \quad (2.2)$$

The number of terms in the two series is  $N$ , and the standard deviation of the  $x_i$  series is  $\sigma_X$ , which is defined as:

$$\sigma_X = \sqrt{\frac{1}{N} \sum_{i=1}^N (x_i - \mu_x)^2}. \quad (2.3)$$

Here  $\mu_x = \frac{1}{N} \sum_{i=1}^N x_i$  is the series mean value, and an analogous expression exists for  $\sigma_Y$ . The correlation function of a time series with a lagged copy of itself is the auto-correlation coefficient of the series. Assume we have built a time series with a lag of one,  $y_i = x_{i-1}$ . Equation 2.1 will be used to calculate the auto-correlation coefficient for this  $y_i$ . For lags of 2 ( $y_i = x_{i-2}$ ), 3 ( $y_i = x_{i-3}$ ), and so on, analogous auto-correlation coefficients can be found. The spectrum of auto-correlation coefficients for several values of the time lag is the auto-correlation function (*ACF*) of  $x_i$ . The auto-correlation function is useful for determining the predictability of a series temporal behavior.

Figure 1 depicts two *ACF* for time series of semi-major axis  $a$  of a regular (left panel) and chaotic (right panel) particle in the Veritas orbital region. The regular particle exhibits a significantly higher proportion of auto-correlation coefficients outside the null hypothesis levels of  $\pm 0.05$  than the chaotic one, especially for time lags greater than 200. On short time scales, it becomes impossible to predict the time behavior of the  $a$  series for the chaotic particle. We can create a chaos indicator built on the *ACF*, the auto-correlation function index (*ACFI*), based on these considerations:

$$ACFI = \frac{1}{i_{fin} - i_{in}} \sum_{i=i_{in}}^{i=i_{fin}} n_i(|R| > 0.05), \quad (2.4)$$

where  $n_i(|R| > 0.05)$  denotes the number of auto-correlation coefficients greater than 5% in absolute value. In our instance  $i_{fin} - i_{in} = 500 - 200 = 300$ , and we only consider

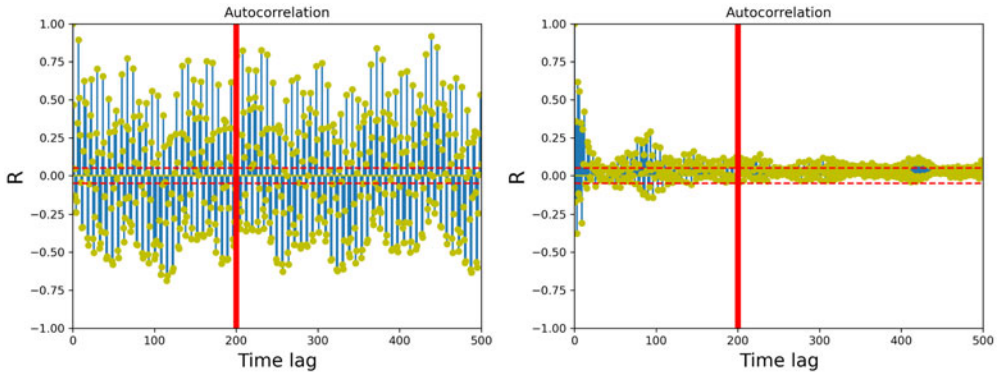


**Figure 1.** The *ACF* of a normal asteroid in the Veritas family orbital region is shown in the left panel. The *ACF* of a somewhat chaotic orbit is shown in the right panel. The vertical line shows a 200 time-step lag. The area between dashed horizontal lines represents the region where auto-correlation coefficients are less than 5% and represents negligible auto-correlation.

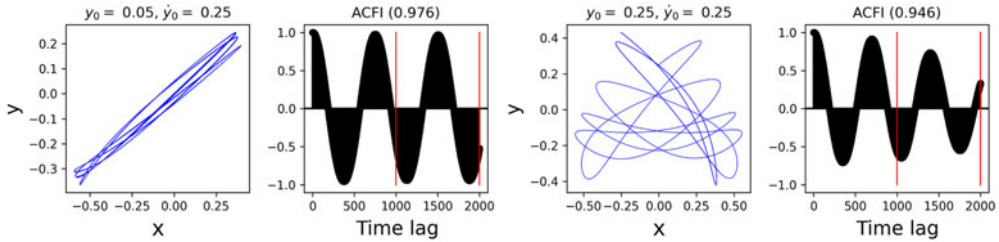


**Figure 2.** A  $(x, y)$  projection of a normal orbit (left panel) and its *ACF*, shown in the panel in the center left position. The values of the  $i_{in}$  and  $i_{fin}$  parameters are represented by the vertical red lines. The panels on the center right and right positions display the same quantities, but for a chaotic orbit.

coefficients between 200 and 500 to avoid include auto-correlation at short time-frames. The values of  $i_{in}$  and  $i_{fin}$  were chosen after experimenting with lower and upper bounds in the ranges of 100 to 300 and 300 to 1000, respectively. Changing either of the given parameters has a maximum effect on *ACFI* values of 0.04 for regular particles and of 0.01 for chaotic ones. By adjusting either parameter, the mean values of *ACFI* are modified by less than 1%.

We will apply *ACFI* to the Hénon-Heiles system in the next section to see how well this method may be utilized to detect chaotic behavior in a well-known system.

### 3. The Hénon-Heiles Hamiltonian system case

The Hamiltonian of the Hénon-Heiles system (*HH*) is:

$$H(x, y, \dot{x}, \dot{y}) = \frac{1}{2}(\dot{x}^2 + \dot{y}^2) + \frac{1}{2}(x^2 + y^2) + x^2y - \frac{1}{3}y^3, \tag{3.1}$$

The Hamiltonian was integrated in such a way that the trajectory passes across the  $x$ -axis 1000 times. A  $(x, y)$  projection of the orbit and the *ACF* of a regular (left side) and chaotic (right side) orbits for this system are shown in figure (2). Here, we set the  $i_{in}$  and  $i_{fin}$  free parameters of *ACFI* to 1000 and 2000, respectively. The *HH* system’s regular orbits have higher *ACFI* values.

We first utilize the Smaller Alignment Index (*SALI*) approach, which uses the area of a parallelogram generated by two deviation vectors in the tangent space of the orbit to

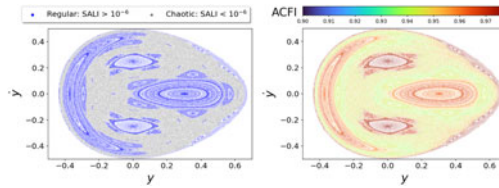


**Figure 3.** The 2D Hénon-Heiles system with  $H = 0.125PSS$ . The *SALI* algorithm is used to classify orbits in the left panel. The *PSS* values of *ACFI* are shown in the right panel.

assess the effect of applying *ACFI* to this system. The *SALI* method’s definition is as follows:

$$\begin{aligned}
 SALI(t) &= \min(d_-, d_+) \\
 d_- &= \left\| \frac{w_1(t)}{\|w_1(t)\|} - \frac{w_2(t)}{\|w_2(t)\|} \right\| \\
 d_+ &= \left\| \frac{w_1(t)}{\|w_1(t)\|} + \frac{w_2(t)}{\|w_2(t)\|} \right\|
 \end{aligned}
 \tag{3.2}$$

$w_1$  and  $w_2$  are two deviation vectors that start off orthogonal and point in two random directions. We refer interested readers to Skokos (2001), Skokos *et al.* (2003), and Skokos *et al.* (2004) for more details on this method.

The Poincaré Surface of Section (*PSS*) in the  $(y, \dot{y})$  plane for the Hénon-Heiles system with Hamiltonian  $H = 0.125$  is shown in figure (3). For all of the orbits evaluated, we set  $x_0$  to 0 and varied  $y_0$  from -0.43 to 0.65 with a 0.001 step. We then changed the value of  $\dot{y}_0$  from -0.5 to 0.5 with a 0.005 step and estimated the value of  $\dot{x}_0$  using eq. (3.1). The *PSS* is made up of the spots on the x-axis where the trajectories cross. On each revolution, each orbit passes over the Poincare section twice, but only the one with positive y velocity is considered. In the *PSS*, a quasi-periodic orbit appears as a set of points on a smooth closed curve. Chaos, on the other hand, will result in scattered locations on the map. The *SALI* approach clearly differentiates between regular and chaotic behavior. In our example, a value of  $SALI = 10^{-6}$  is used to distinguish between the two types of motion (see left panel of Fig. (3)).

After that, we compute *ACFI* for each orbit in the system. In the right panel of Fig. 3, we show our findings. A greater value of *ACFI* is associated with most regular behavior, and the two techniques appear to give qualitatively identical outcomes. The advantage of *SALI* for this system is that it can distinguish between chaotic and regular behavior with a single value, whereas the *ACFI* distribution is more subtle. We can see that, unlike the *SALI* method, there is no distinct value distinguishing the regular and chaotic motions; however, a high value of this indicator can characterize the majority of the regular motion in the system. With a very low *ACFI* value, certain small islands of regular orbits appear on the map, and the *SALI* indicator detects these as regular zones. This might alter if integration times were extended. However, exploring these areas in greater depth is not the main focus of our research. Despite this, *ACFI* appears to be able to recognize all of the chaotic regions in the *SALI PSS*.

More detailed results on the theory and applications to small bodies dynamics of *ACFI* can be found at Carruba *et al.* (2021).

### Acknowledgements

We are grateful to the reviewer of this work, Dr. Cătălin Gales, for helpful comments and suggestions. We would like to thank the Brazilian National Research Council (CNPq), that supported VC with the grant 301577/2017-0, and WB with the PIBIC grant

121889/2020-3, The Coordination for the Improvement of Higher Education Personnel (CAPES), for supporting SA with the grant 88887.374148/2019-00. RD is supported by the São Paulo Research Foundation (FAPESP, Grant 2016/024561-0). VC, RD, and WB are part of "Grupo de Dinâmica Orbital & Planetologia (GDOP)" (Research Group in Orbital Dynamics and Planetology) at UNESP, campus of Guaratinguetá. This is a publication from the MASB (Machine-learning applied to small bodies, <https://valeriocarruba.github.io/Site-MASB/>) research group.

#### 4. Code availability

The Python code for identifying chaotic behavior is available at the GitHub repository: <https://github.com/valeriocarruba/ACFI-Chaos-identification-through-the-autocorrelation-function-indicator>.

#### References

- Carruba V., Aljbaae S., Domingos R. C., Huaman M., Barletta W., (2021) *CMDA*, 133, A38.
- Frahm KM., Fleckinger R., Shepelyansky DL. (2004) *European Physical Journal D* 29(1), 139.
- Lewis-Swan RJ., Safavi-Naini A., Bollinger JJ., Rey AM. (2019) *Nature Communications* 10, 1581.
- Pearson K. (1895) *Proceed. Royal Society of London, Series I*, 58, 240.
- Pellegrini F., Montagero S. (2007) *Physical Review A* 76(5):052327.
- Skokos CH. (2001) *Journal of Physics A Mathematical General* 34, 10029.
- Skokos C., Antonopoulos C., Bountis T., Vrahatis M. (2003) *Progress of Theoretical Physics Supplement* 150, 439.
- Skokos C., Antonopoulos C., Bountis TC., Vrahatis MN. (2004) *Journal of Physics A Mathematical General* 37, 6269.
- Skokos CH., Gottwald GA., Laskar J. (2016) *Lecture Notes in Physics, Berlin Springer Verlag* 915:E1.